NACA

RESEARCH MEMORANDUM

THE EFFECT OF ASPECT RATIO ON THE SUBSONIC AERODYNAMIC CHARACTERISTICS OF WINGS WITH NACA 65_1-210 SECTIONS

By Warren H. Nelson and Albert L. Erickson

Ames Aeronautical Laboratory
Moffett Field, Calif.

NATIONAL ADVISORY COMMITTEE FOR AERONAUTICS

WASHINGTON
February 3, 1950

NATIONAL ADVISORY COMMITTEE FOR AERONAUTICS

RESEARCH MEMORANDUM

THE EFFECT OF ASPECT RATIO ON THE SUBSONIC AERODYNAMIC CHARACTERISTICS OF WINGS WITH NACA 65_1-210 SECTIONS

By Warren H. Nelson and Albert L. Erickson

SUMMARY

The results of tests of four model wings of aspect ratios 1, 2, 4, and 6, employing NACA 65_1-210 sections, are presented. The wings had taper ratios of 0.4 and 3° dihedral. Decreasing the aspect ratio resulted in an increase in the Mach number of drag and lift divergence. The experimental lift-curve slope is compared with that predicted by theory. The measured drags were low compared to the drags of wings having the same sections but higher aspect ratios reported in NACA Rep. 877, 1947, possibly due to the interference effects of the balance housing, causing transition to occur well back on the wing.

INTRODUCTION

Previous work (reference 1) has shown the possible benefits of low-aspect-ratio wings for transonic flight due to an increase in the Mach number of lift and drag divergence. The purpose of the work reported herein was to evaluate these benefits at larger Reynolds numbers. These Reynolds numbers varied from 4,700,000 for the wing with the smallest chord at 0.4 Mach number to 10,700,000 for the wing with the largest chord at 0.9 Mach number. A study of experimental and theoretical lift-curve slopes using the Prandtl-Glauert law and the methods outlined in references 2 and 3 is included. A comparison is made of the theoretical frictional drags and the experimental minimum drags.

SYMBOLS

The following symbols are used in this report:

A aspect ratio $\left(\frac{b^2}{S}\right)$

C_D drag coefficient $\left(\frac{\text{drag}}{qS}\right)$

C_L lift coefficient $\left(\frac{\text{lift}}{qS}\right)$

C_m pitching-moment coefficient about quarter-chord line $\left(\frac{\text{pitching moment}}{qS\bar{c}}\right)$

M Mach number

S wing area, square feet

V velocity, feet per second

b wing span, feet

c chord, feet

$\bar{c}$ mean aerodynamic chord $\left(\frac{\int_0^{b/2} c^2\,dy}{\int_0^{b/2} c\,dy}\right)$, feet

$dC_L/d\alpha$ lift-curve slope, per degree

q dynamic pressure $\left(\frac{1}{2}\rho V^2\right)$, pounds per square foot

y spanwise distance, feet

α angle of attack of wing reference plane, degrees

ρ mass density, slugs per cubic foot

MODELS AND TEST TECHNIQUE

These tests were conducted in the Ames 16-foot high-speed wind tunnel using four model wings having aspect ratios of 1, 2, 4, and 6. The wings all had NACA 65_1-210 sections with a uniform chordwise load distribution (a = 1), taper ratios of 0.4, 3° dihedral, and no twist.

The 25-percent-chord lines had no sweep. The basic dimensions and plan forms of the wings are given in figure 1.

The model wings were supported on a sting as shown in figure 2. The forces were measured by a strain-gage balance mounted inside the models so that there were no direct tare forces. A body was required to fair in the strain-gage balance used in measuring the forces. Due to the size of the balance, the body could not be buried completely in the wings.

Constriction corrections were applied to the tunnel-empty calibration according to the methods of reference 4. The data were corrected for tunnel-wall effects in the manner described in reference 5. No base-pressure corrections were made. The static-pressure gradient in the wind tunnel was not sufficient to give a measurable buoyancy correction.

The maximum speeds obtained in these tests were limited either by balance strength or blocking effects. The variation of test Reynolds number with Mach number for all the wings tested is shown in figure 3.

A drag study is included which involved using the liquid-film method, described in reference 6, and fixing transition. Transition was fixed by means of 3/16-inch-wide strips of No. 60 grit carborundum.

RESULTS AND DISCUSSION

Lift, Drag, and Pitching Moment

The aerodynamic characteristics of the wings for Mach numbers from 0.4 to 0.9 are presented in figures 4 to 6. Figure 4 shows the lift coefficient as a function of angle of attack for the four wings tested. The nonlinearity of the lift curves for the low-aspect-ratio wings is apparent. The drag characteristics as a function of lift are shown in figure 5. The minimum drags measured were lower than expected. The increased induced-drag effects are apparent in the high rate of drag rise with increased lift as the aspect ratio was reduced. The moment coefficients as a function of lift coefficient are shown in figure 6. In general, for the wings with aspect ratios of 1 and 2, the moment curves indicate an increase in stability with increasing lift coefficient. The moment curves for the wings with aspect ratios of 4 and 6 showed a small increase in stability with increasing Mach number.

Lift-Curve Slope

As the aspect ratio decreased, the effect of Mach number on the lift-curve slope decreased (fig. 7). This is to be expected as the three-dimensional effects become more predominant. It is shown in reference 7 that the pressure coefficient at the surface of a slender streamline body of revolution in a uniform stream of a compressible fluid is nearly independent of Mach number as opposed to the two-dimensional, thin, streamline body where the pressure coefficients increase by $1/(1-M^2)^{1/2}$, the familiar Prandtl-Glauert formula based on the linear perturbation theory. There are methods available for predicting the effect of compressibility for various aspect ratios based on the linear perturbation theory. Two of these methods (references 2 and 3) have been compared with the experimental results. The other theoretical curves in figure 7 are based on the Prandtl-Glauert two-dimensional correction $1/(1-M^2)^{1/2}$. The lift-curve slopes predicted for zero Mach number are taken from reference 8, and the theories are applied from this base. The lift-curve slope for two-dimensional incompressible flow used in the theory of reference 2 was obtained from reference 9. The theoretical rate of change of lift-curve slope with Mach number calculated from reference 2 agrees fairly well with the experimentally determined values for the lower aspect ratios below the divergence Mach number, but, for an aspect ratio of 6, the theoretical values are generally less than the experimental ones. The two-dimensional Prandtl-Glauert law does not give sufficient correction at Mach numbers above 0.7 for the wing of aspect ratio 6, but it overcorrects for the lower aspect ratios. This disagreement is due to the breakdown of the linear perturbation theory at high Mach numbers for airfoils of finite thickness, as has been shown by other tests (reference 10).

Drag Divergence

The benefit of increased Mach number of divergence for the low-aspect-ratio wings was obtained at the expense of increased induced drag as shown in figure 8. The magnitude of the drag coefficient at 0.4 lift coefficient for aspect ratios of 1 and 2 was extremely high, indicating that the Mach number and lift coefficient for operation is of critical importance in choosing the aspect ratio.

Decreasing the aspect ratio also can result in increases in the drag-divergence Mach number because the thickness-to-chord ratio of the wing also can be reduced. For the same root stress, the wing thickness can be reduced approximately as the square root of the ratio of the aspect ratios. If the same loading is assumed and wings from the present series of tests are compared, a 4-percent-thick wing with an aspect ratio of 1 will have the same root stress as a 10-percent-thick wing with an aspect ratio of 6. This decrease in thickness would increase the critical Mach number, based on two-dimensional airfoil data, by 0.04 to 0.06 (reference 9).

Minimum Drag

The measured minimum drags are exceptionally low, which was thought to be due to transition occurring unusually far back on the wings. Consequently, a series of tests was made of the aspect-ratio-2 wing, with and without fixed transition. The results, along with calculated frictional drag coefficients (reference 11), are shown in table I. To ascertain the chord position at which transition was normally taking place, a liquid film was applied to the aspect-ratio-2 wing. The film evaporated first in the turbulent area, leaving a contrast due to the change in reflectivity of the wing as is shown in figure 9. It was estimated from these photographs that, for a Mach number of 0.7 and at minimum drag, the average transition point on the upper surface of this wing was at about 65 percent of the chord on the outer 50 percent of the span. The inner portion of the span did not show any clear turbulent area except where minute surface irregularities caused the usual wedge-shaped transition areas forward of the 50-percent-chord line. On the lower surface, the liquid film indicated that transition was occurring at about 55-percent chord. A test was made with transition fixed at 65 percent of the chord on both upper and lower surfaces. The results (table I) show a higher drag than for the normal wing, indicating that transition was occurring aft of 65 percent of the chord on at least part of the smooth wing. The drag directly due to the rough strip was estimated to be less than 1 percent of the total drag. As mentioned earlier, the liquid film indicated transition might have been occurring aft of 65 percent of the chord on the inner portion. In order to check this indication, the transition-fixing roughness was removed from the inner 50 percent of the span on the upper surface, and the drag then agreed with the smooth-wing drag. It is apparent from these results that transition on the upper surface of the inner portion of the span was occurring aft of 65 percent of the chord on the smooth wing. This far aft position of transition was possibly due to favorable interference effects of the body in reducing the pressure gradients on the inner portion of the wing. This hypothesis could explain why the minimum drags are lower than those measured in reference 10.

Additional drag measurements were made with transition fixed forward of the normal position, and the results are included in table I. The additional drag measurements for various positions of fixed transition are in good agreement with frictional-drag calculations. Included in table I are the results of tests with the wing surface polished. A reduction in drag coefficient of about 0.0004 was realized for this polished condition when compared to the wing in the normal smooth condition.

The absolute magnitude of the drag coefficients may be in error by an amount equal to the undetermined base-pressure correction; however, the differences between drag coefficients presented are believed to be reliable.

Pitching Moment

The pitching-moment coefficients are presented as functions of Mach number in figure 10. The low-aspect-ratio wings (1 and 2) had the smallest changes up to the Mach number of divergence. The pitching-moment coefficients for the wings of aspect ratios 2, 4, and 6 become more negative above the critical Mach number.

CONCLUDING REMARKS

These high Reynolds number tests substantiate results from previous low Reynolds number tests in showing that the Mach number of lift and drag divergence was increased by decreasing aspect ratio.

None of the variations of the theory used for predicting the change of lift-curve slope with Mach number was applicable for all aspect ratios tested; however, reference 3 does hold well for aspect ratios 1, 2, and 4 for Mach numbers below the divergence.

Low minimum drags were measured, compared to those reported in NACA Rep. 877, 1947, and it is shown that they can be explained by the fact that transition occurred well behind the 50-percent-chord point. The delayed transition was possibly due to the interference effects of the wing-support system.

Ames Aeronautical Laboratory,
National Advisory Committee for Aeronautics,
Moffett Field, Calif.

REFERENCES

1. Stack, John, and Lindsey, W. F.: Characteristics of Low-Aspect-Ratio Wings at Supercritical Mach Numbers. NACA TN 1665, 1948.

2. Young, A. D.: Note on the Effect of Compressibility on the Lift Curve Slope of a Wing of Finite Span. TN Aero. 1250, R.A.E. (British), 1943.

3. Dickson, R.: The Relationship Between the Compressible Flow Round a Swept-Back Aerofoil and the Incompressible Flow Round Equivalent Aerofoils. Aero. 2146, R.A.E. (British), 1946.

4. Herriot, John G.: Blockage Corrections for Three-Dimensional-Flow Closed-Throat Wind Tunnels, With Consideration of the Effect of Compressibility. NACA RM A7B28, 1947.

5. Silverstein, Abe, and White, James A.: Wind-Tunnel Interference with Particular Reference to Off-Center Positions of the Wing and to the Downwash at the Tail. NACA Rep. 547, 1935.

6. Gray, W. E.: A Simple Visual Method of Recording Boundary Layer Transition (Liquid Film). TN Aero. 1816, R.A.E. (British), 1946.

7. Herriot, John G.: The Linear Perturbation Theory of Axially Symmetric Compressible Flow with Application to the Effect of Compressibility on the Pressure Coefficient at the Surface of a Body of Revolution. NACA RM A6H19, 1947.

8. DeYoung, John: Theoretical Additional Span Loading Characteristics of Wings with Arbitrary Sweep, Aspect Ratio, and Taper Ratio. NACA TN 1491, 1947.

9. Abbott, Ira H., Von Doenhoff, Albert E., and Stivers, Louis S., Jr.: Summary of Airfoil Data. NACA Rep. 824, 1945.

10. Hamilton, William T., and Nelson, Warren H.: Summary Report on the High-Speed Characteristics of Six Model Wings Having NACA 65-Series Sections. NACA Rep. 877, 1947.

11. Hall, Charles F., and Fitzgerald, Fred F.: An Approximate Method for Calculating the Effect of Surface Roughness on the Drag of an Airplane. NACA RM A7B24, 1947.

TABLE I. – MINIMUM DRAG COEFFICIENTS FOR THE ASPECT-RATIO-2 WING

Mach number	Type of data	Wing in normal condition (Theory for transition at 0.65c on upper surface and 0.55c on lower surface)	Transition fixed at 0.65c	Transition fixed at 0.65c on outer half of span on the upper surface	Transition fixed at 0.50c	Transition fixed at 0.35c	Transition fixed at 0.20c	Polished wing	Reynolds number (millions)
0.4	Exper.	0.0038	0.0043	0.0037	0.0046	0.0051	0.0060	0.0034	5.60
	Theory	.0040	---	---	.0045	.0053	.0061	---	
.6	Exper.	.0036	.0042	.0037	.0043	.0047	.0051	.0032	7.24
	Theory	.0038	---	---	.0042	.0050	.0058	---	
.75	Exper.	.0031	.0040	---	.0039	.0041	.0049	.0029	8.20
	Theory	.0037	---	---	.0042	.0050	.0057	---	
.85	Exper.	.0061	.0052	---	.0055	.0064	.0063	.0046	8.35

NACA

Plan form	Aspect ratio	Area (sq ft)	Span (ft)	$\bar{c}$ (ft)	Root chord (ft)	Tip chord (ft)
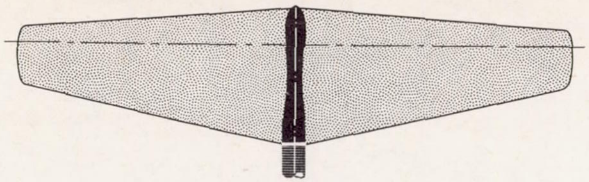	6	16.67	10.00	1.770	2.381	0.952
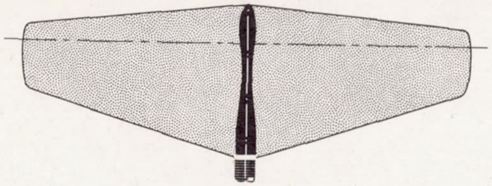	4	16.00	8.00	2.122	2.857	1.143
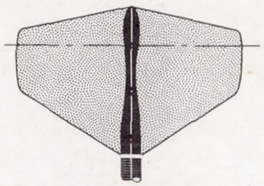	2	8.00	4.00	2.122	2.857	1.143
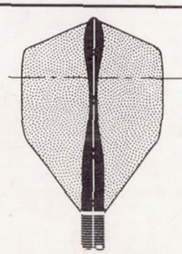	1	6.25	2.50	2.653	3.571	1.429

Figure 1.- Dimensions and plan forms of the model wings.

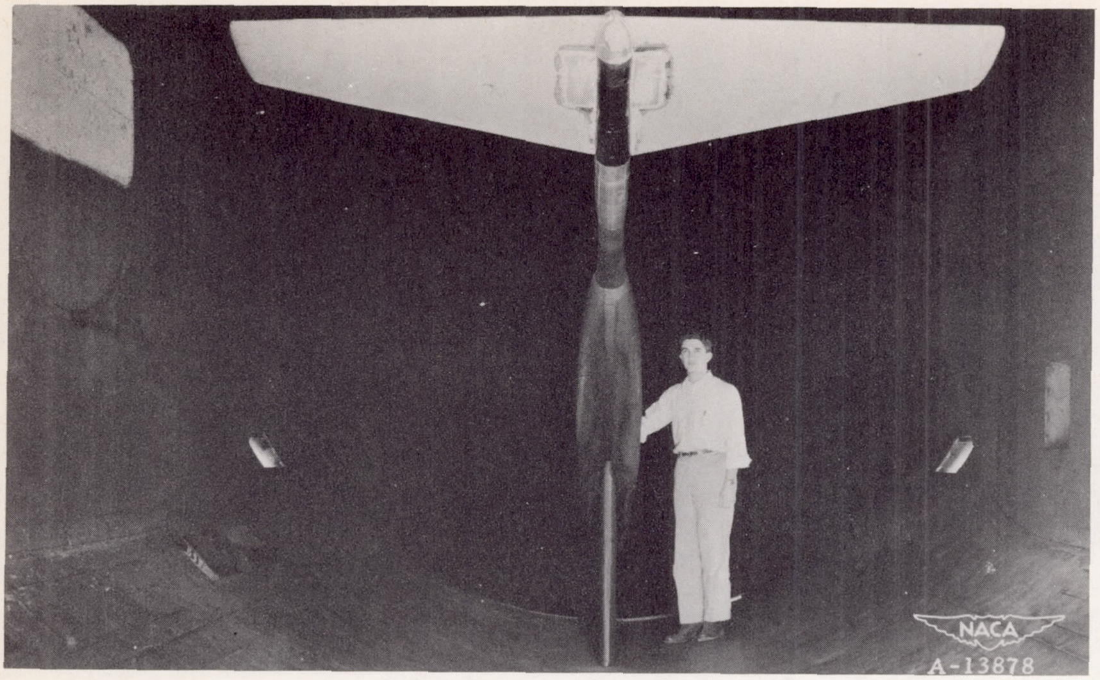

(a) Front view.

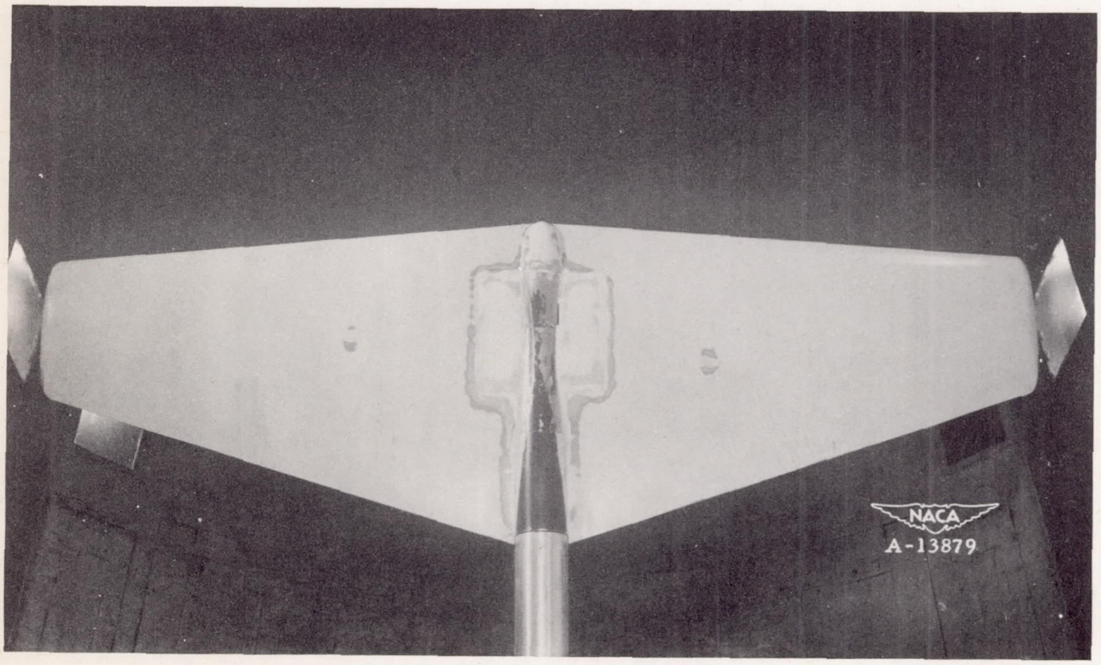

(b) Plan view.

Figure 2.- Method of mounting model wings.

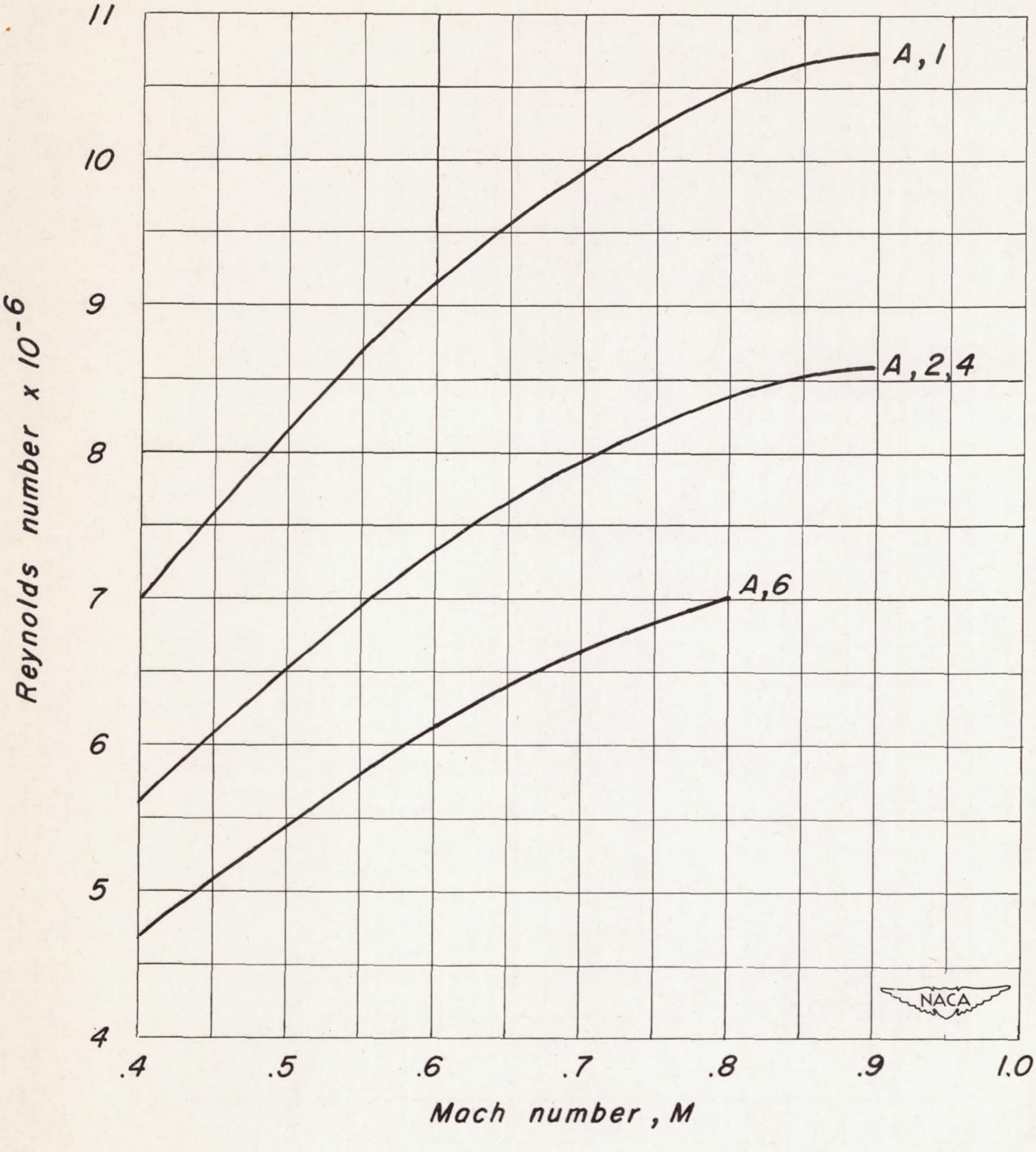

Figure 3.–Variation of Reynolds number with Mach number for the model wings.

CONFIDENTIAL

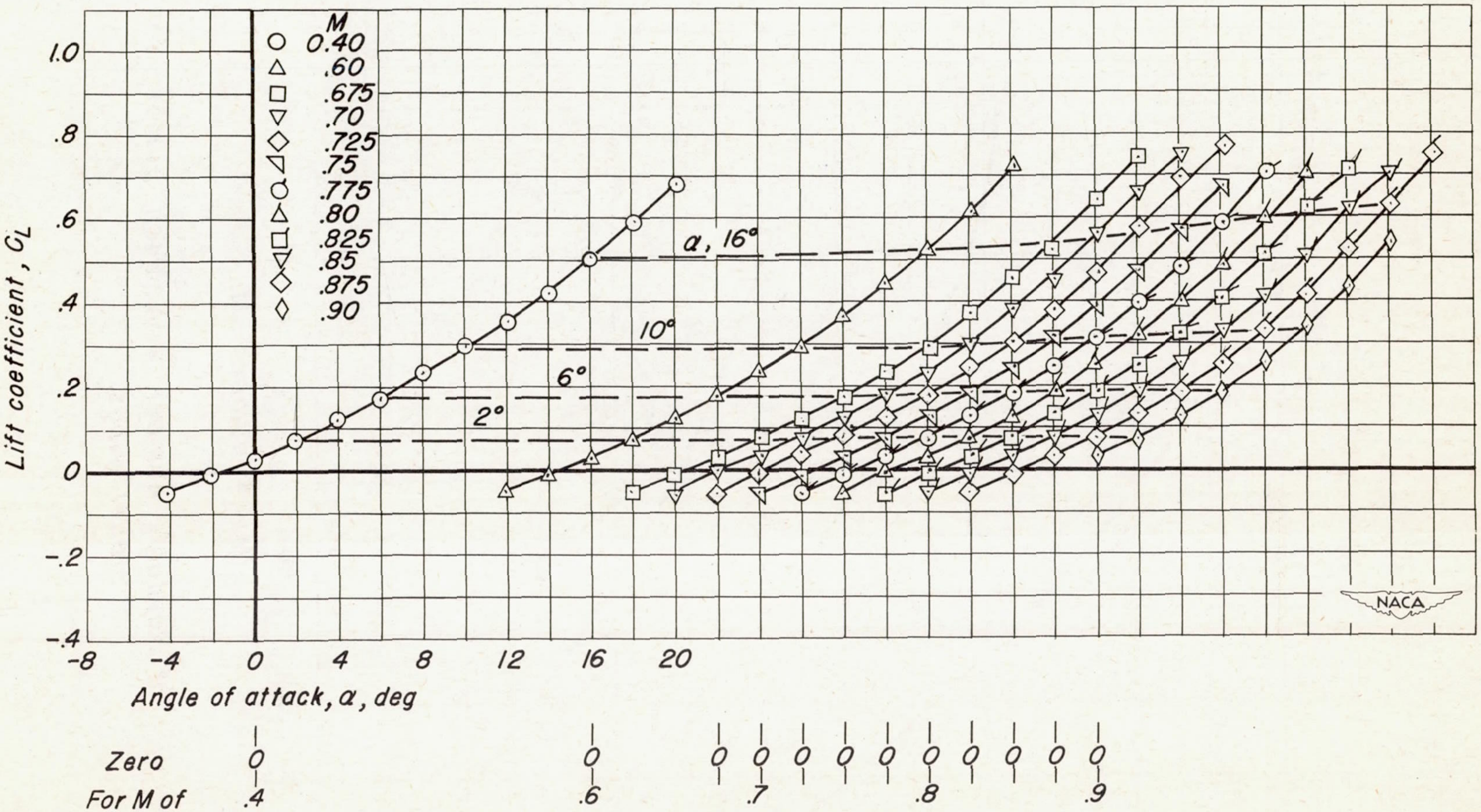

(a) Aspect ratio 1.

Figure 4.– Variation of lift coefficient with angle of attack.

CONFIDENTIAL

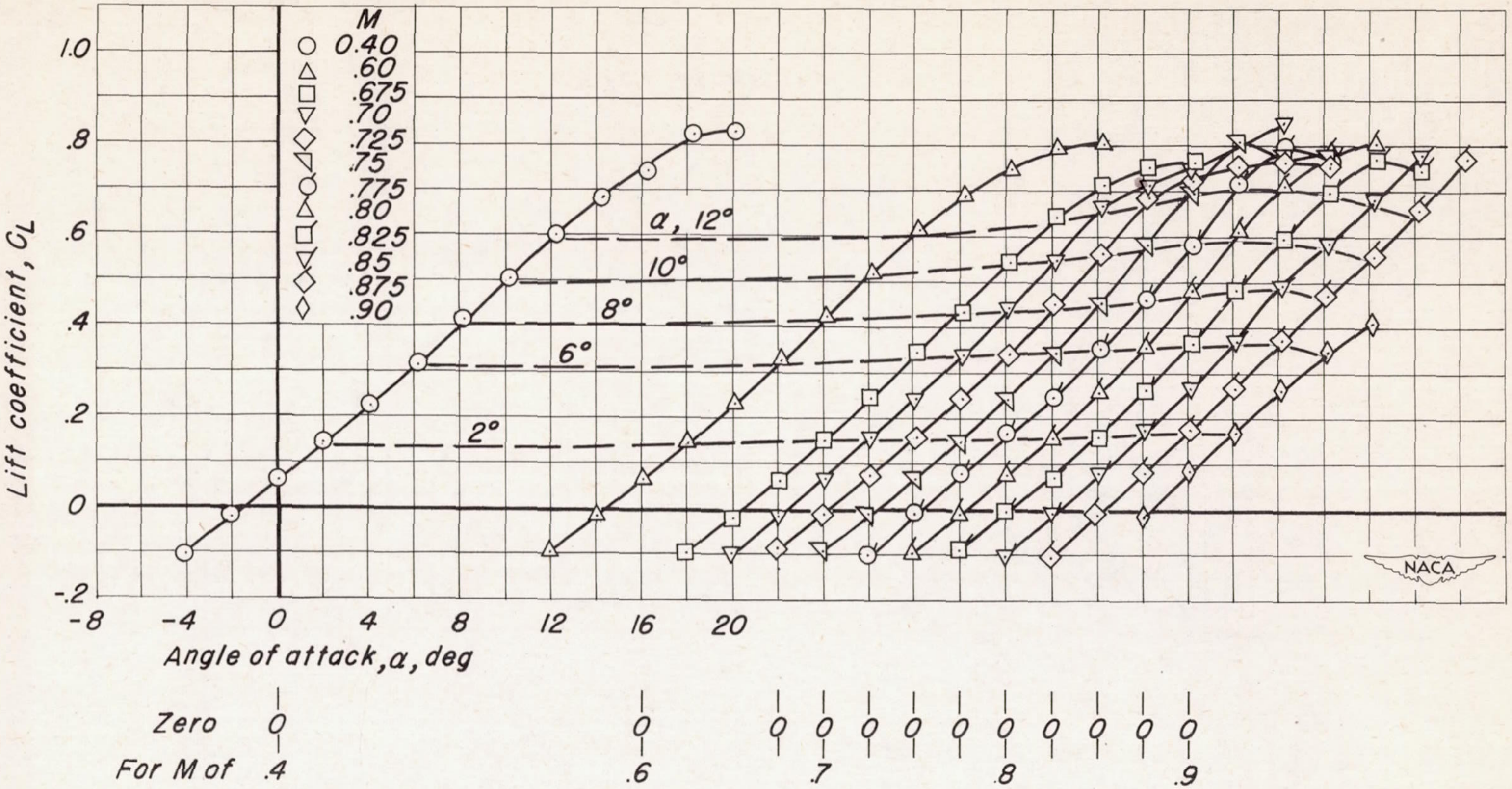

(b) Aspect ratio 2.

Figure 4.—Continued

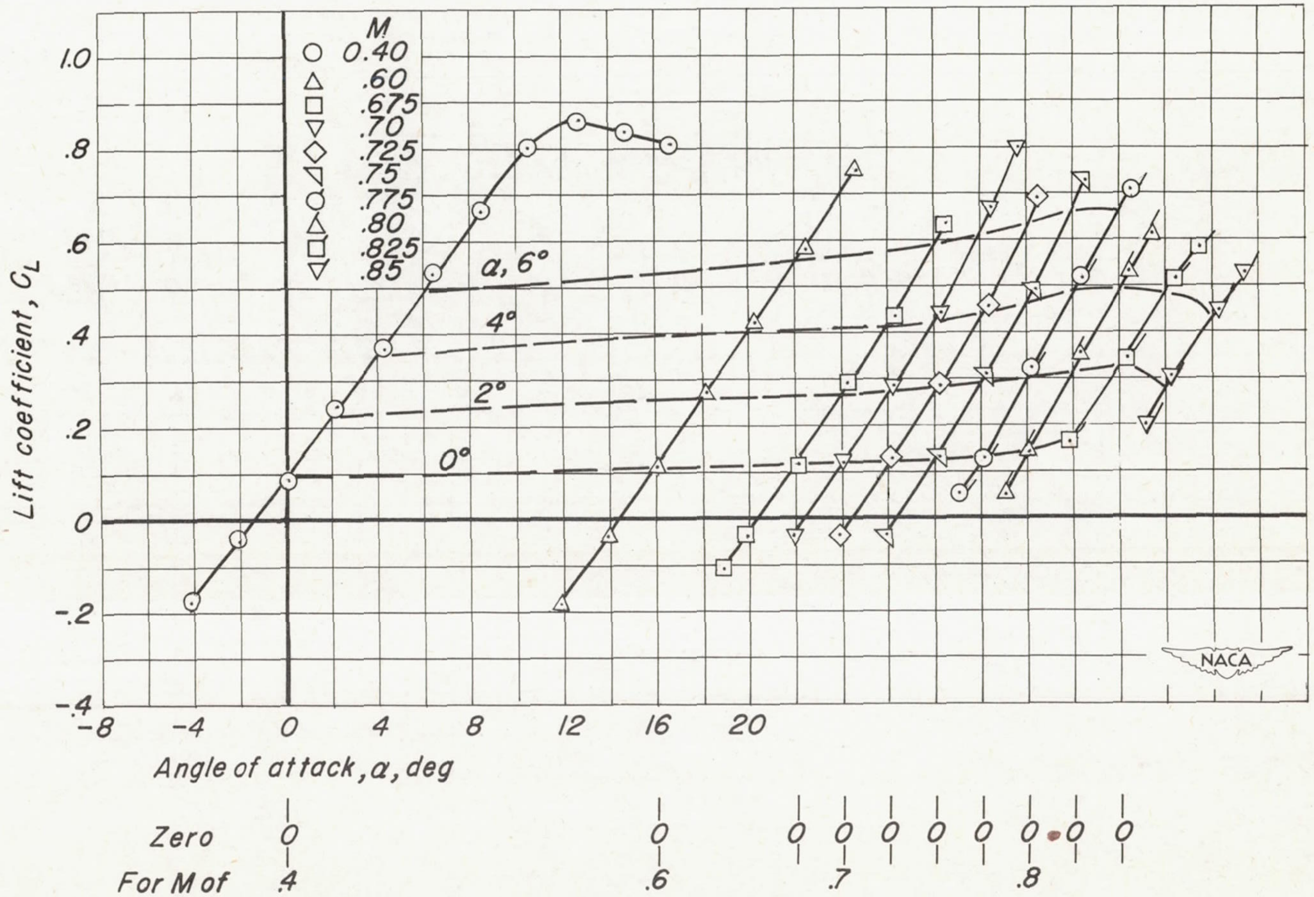

(c) Aspect ratio 4.

Figure 4.—Continued.

CONFIDENTIAL

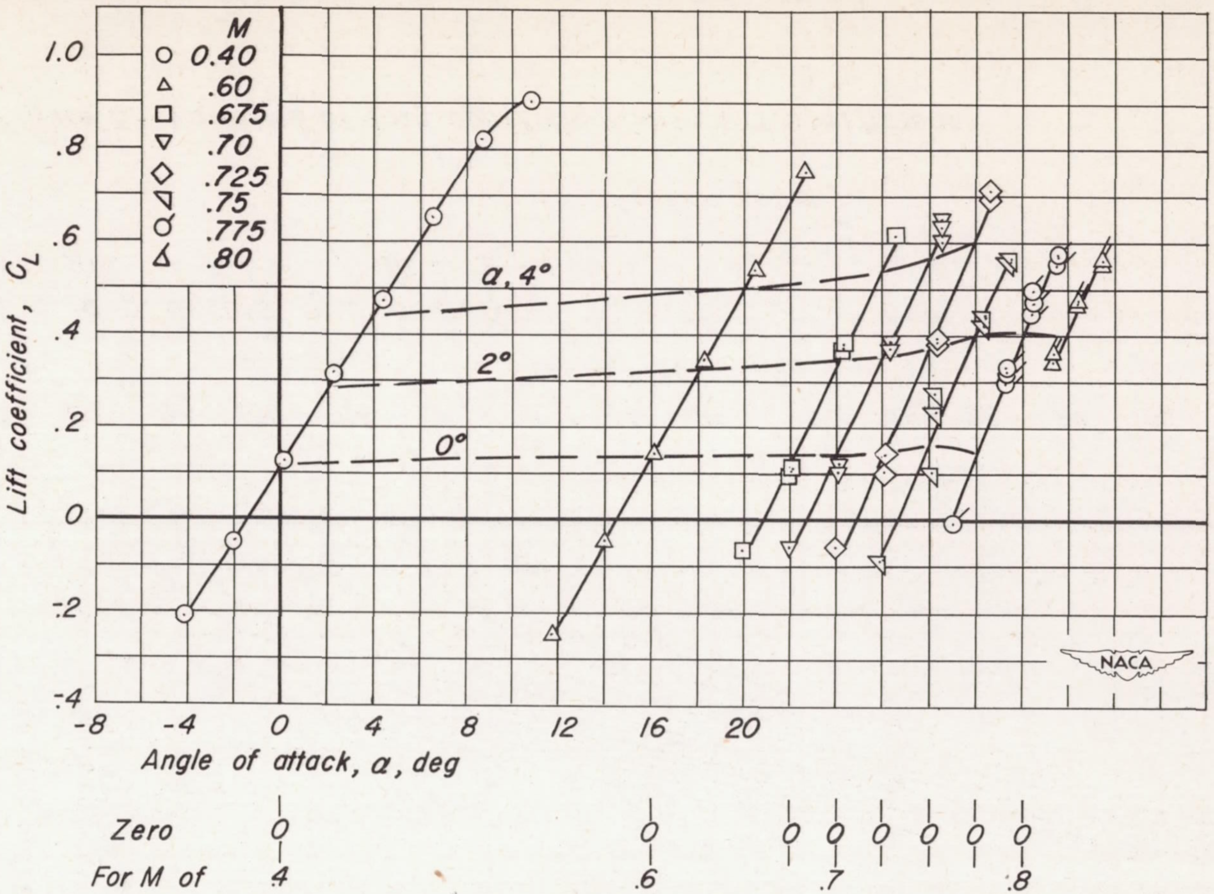

(d) Aspect ratio 6.

Figure 4.–Concluded.

CONFIDENTIAL

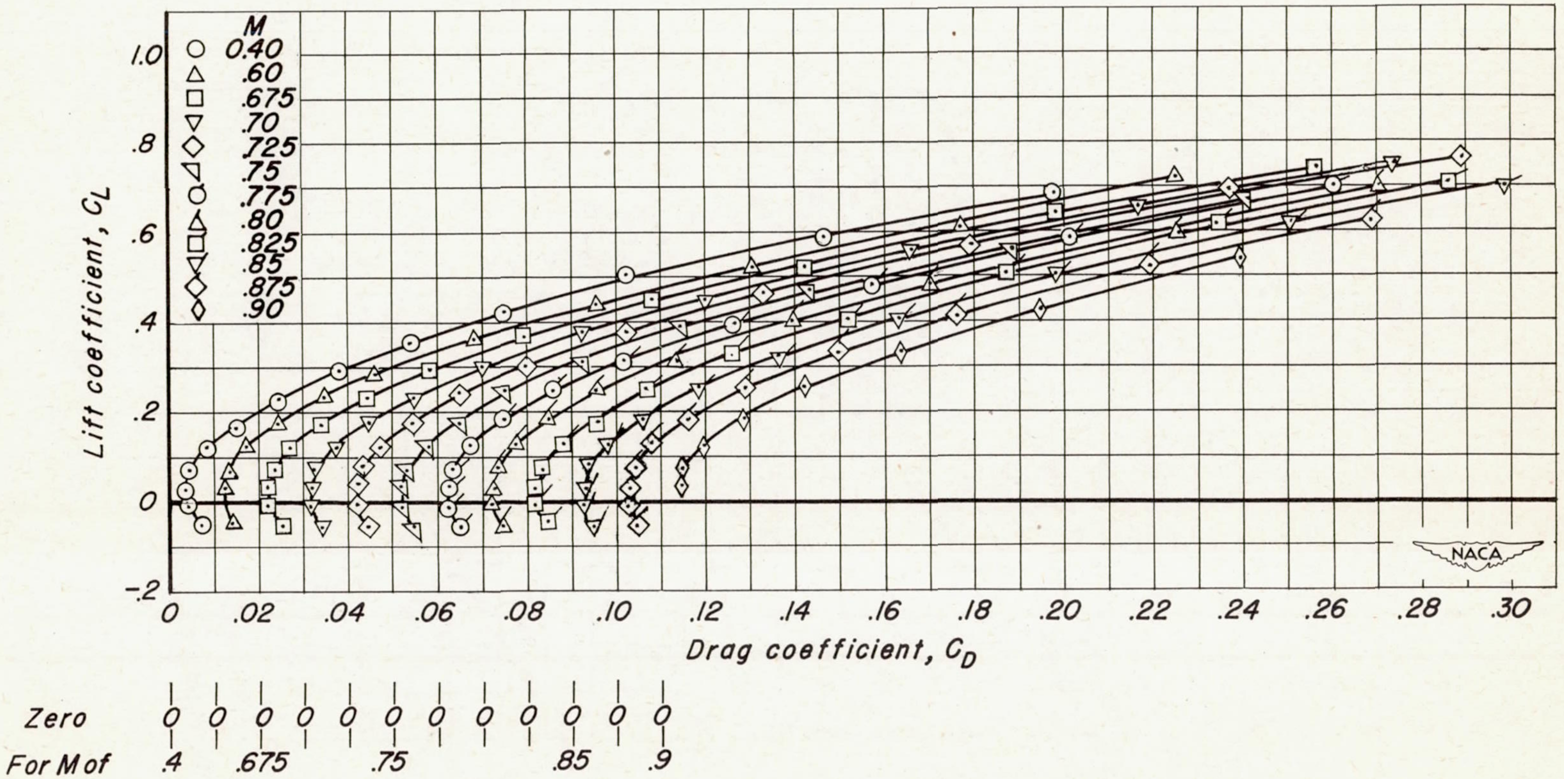

(a) Aspect ratio 1.

Figure 5.- Variation of drag coefficient with lift coefficient.

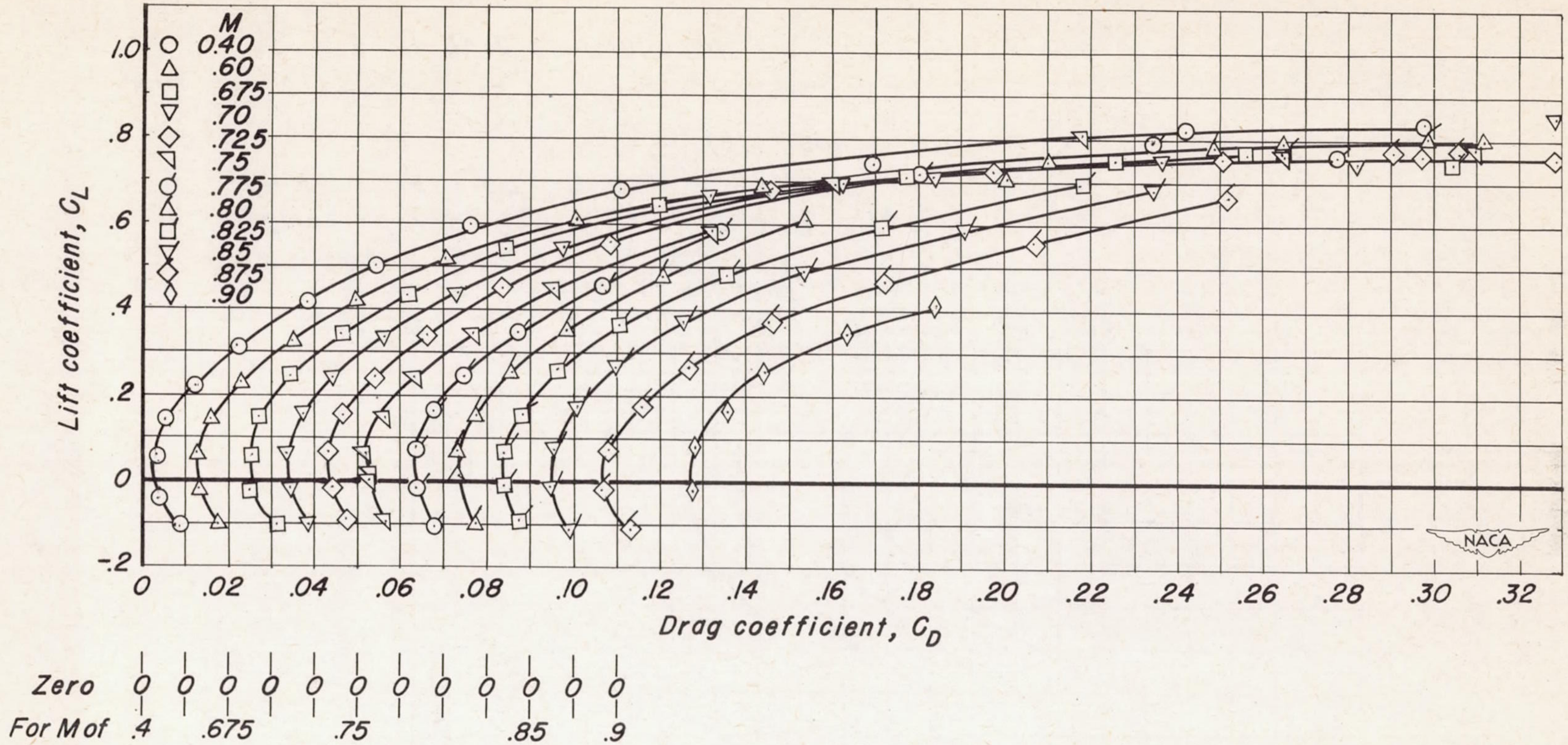

(b) Aspect ratio 2.

Figure 5.– Continued.

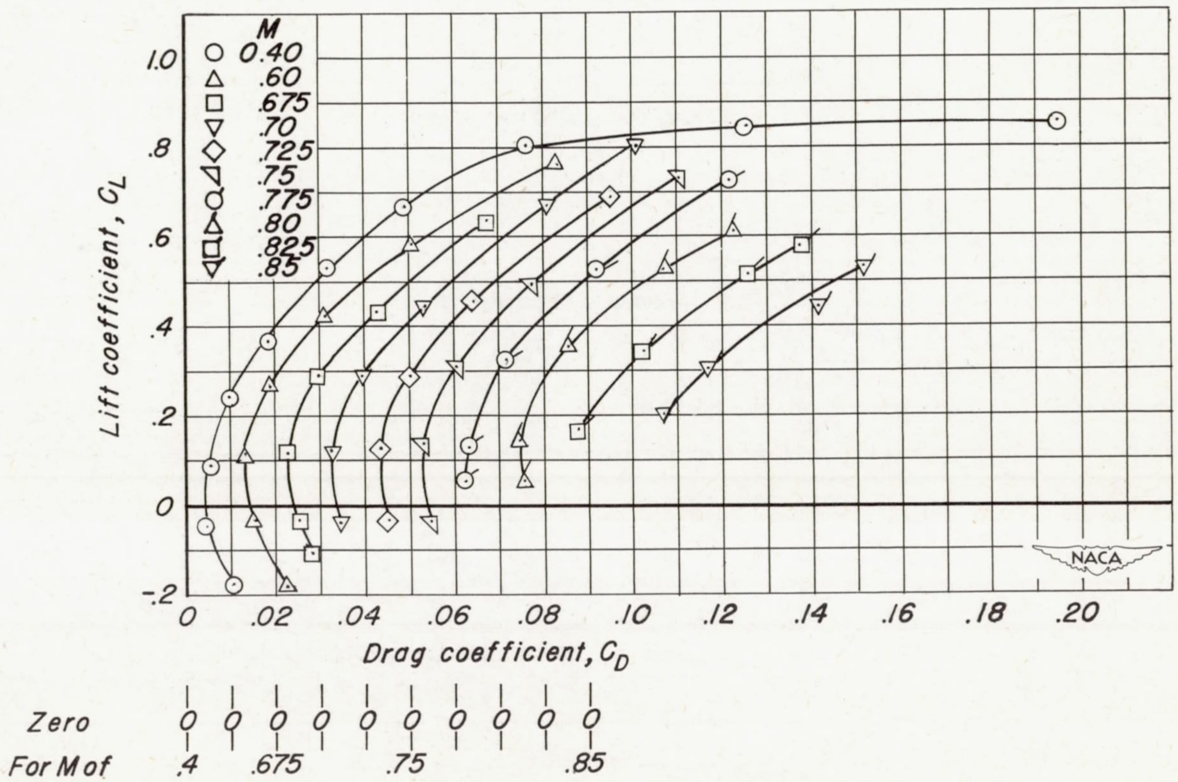

(c) Aspect ratio 4.

Figure 5.—Continued.

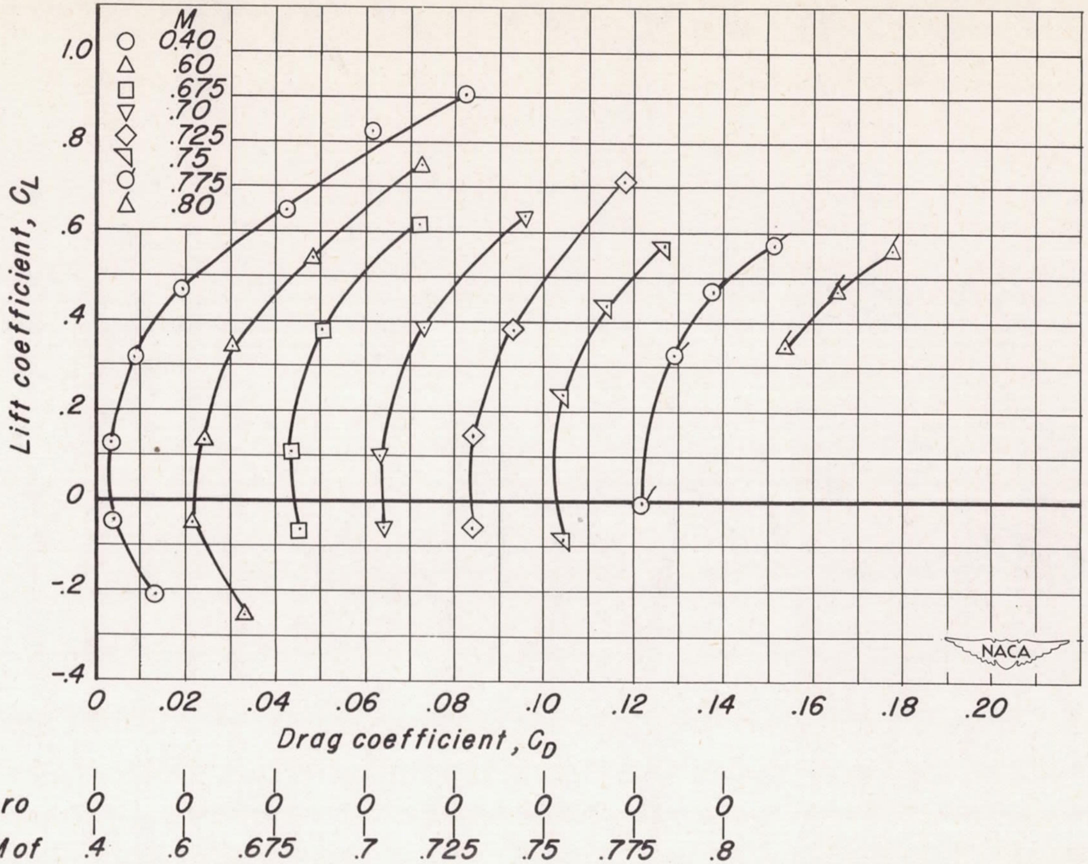

(d) Aspect ratio 6.

Figure 5.– Concluded.

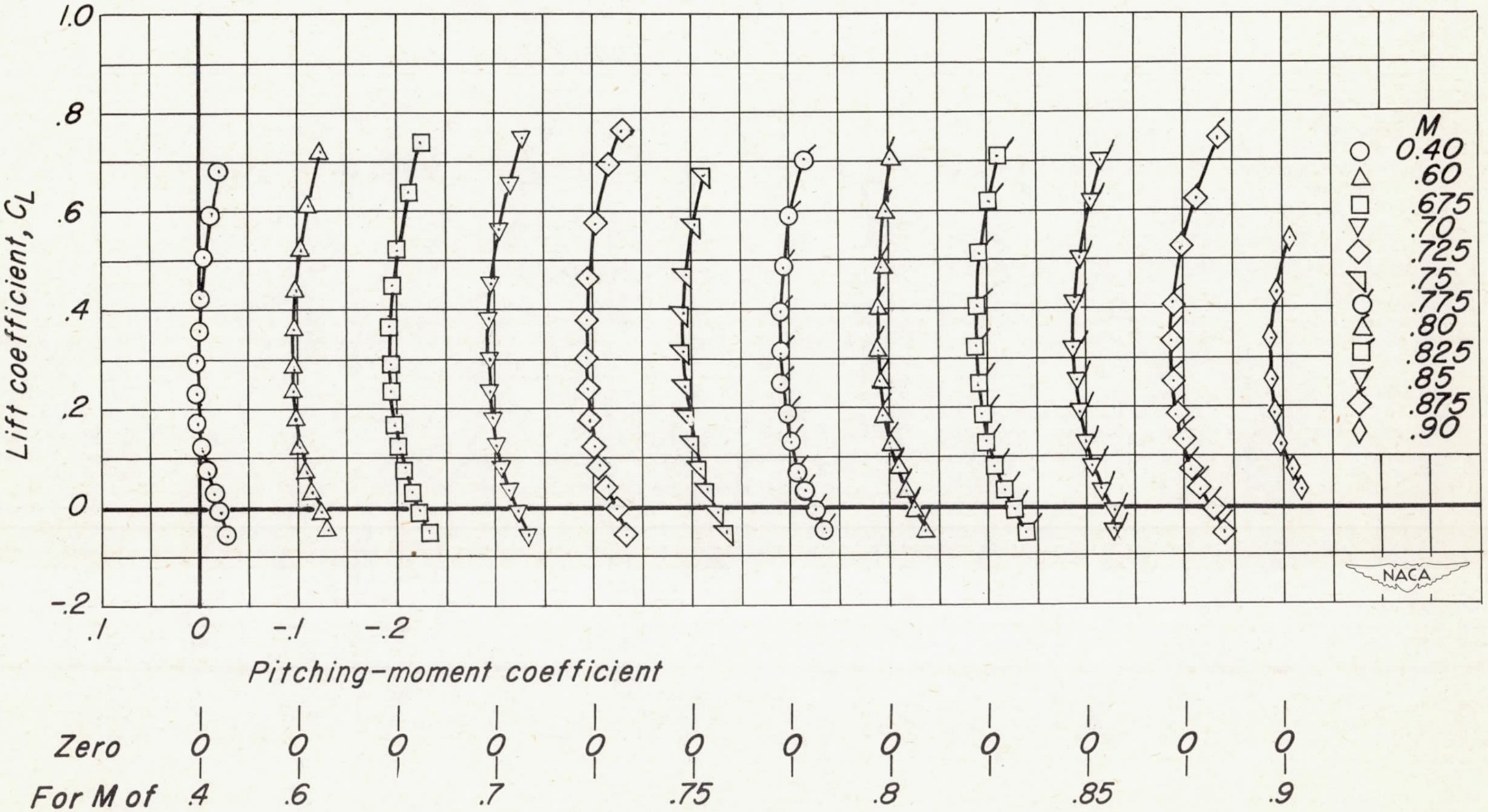

(a) Aspect ratio 1.

Figure 6.-Variation of pitching-moment coefficient with lift coefficient.

CONFIDENTIAL

CONFIDENTIAL

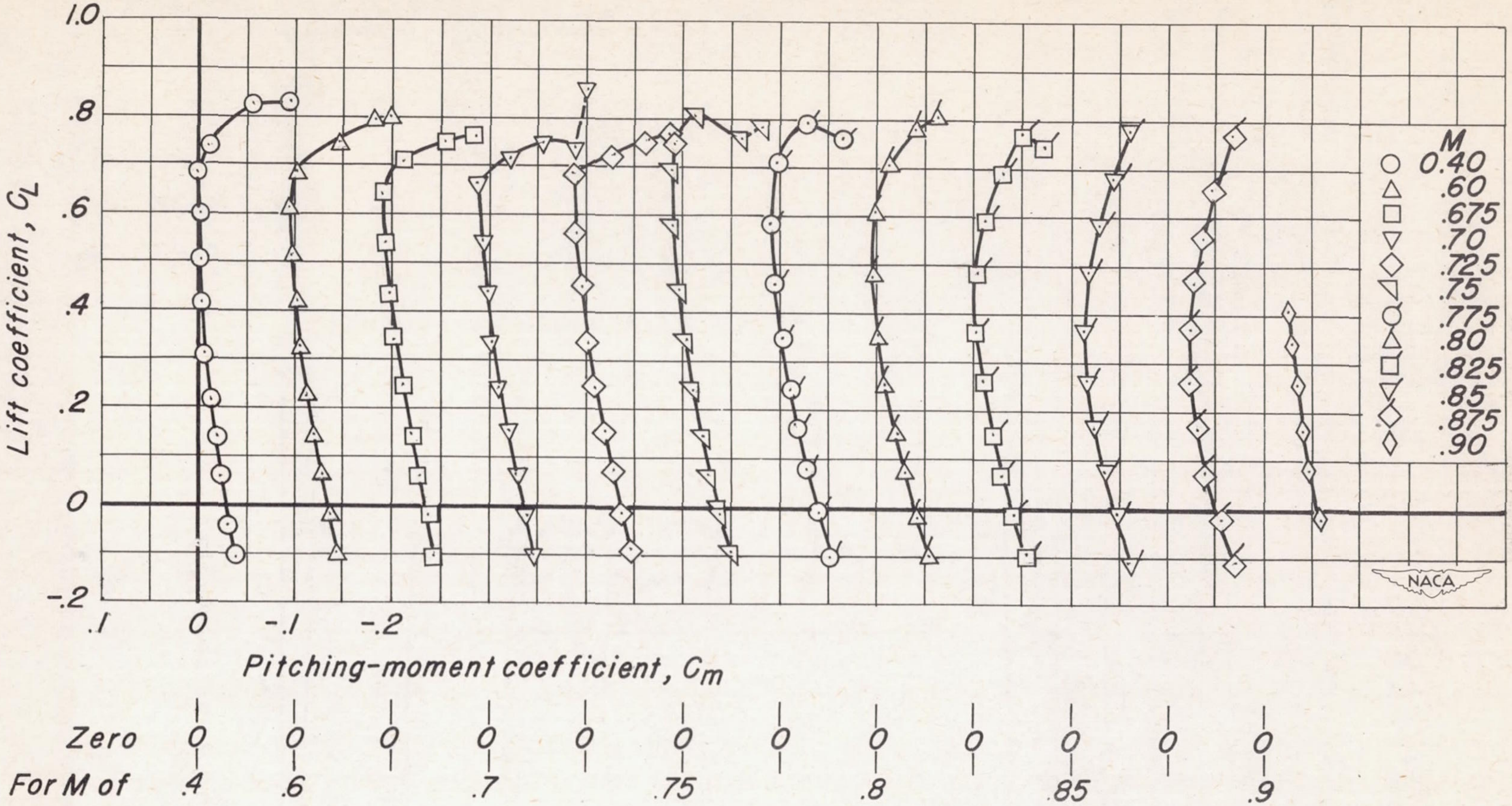

(b) Aspect ratio 2.

Figure 6.– Continued.

CONFIDENTIAL

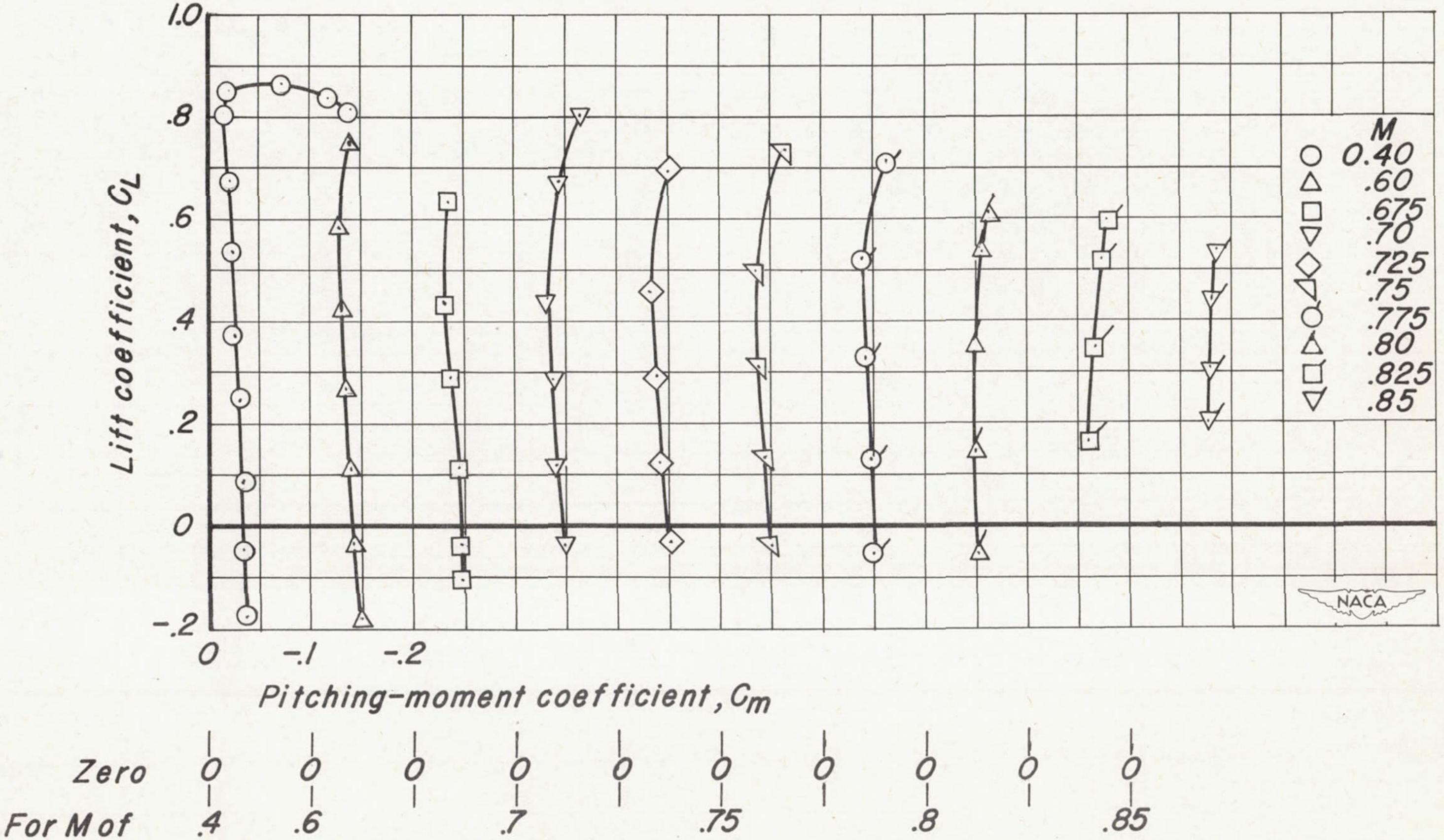

(c) Aspect ratio 4.

Figure 6.–Continued.

CONFIDENTIAL

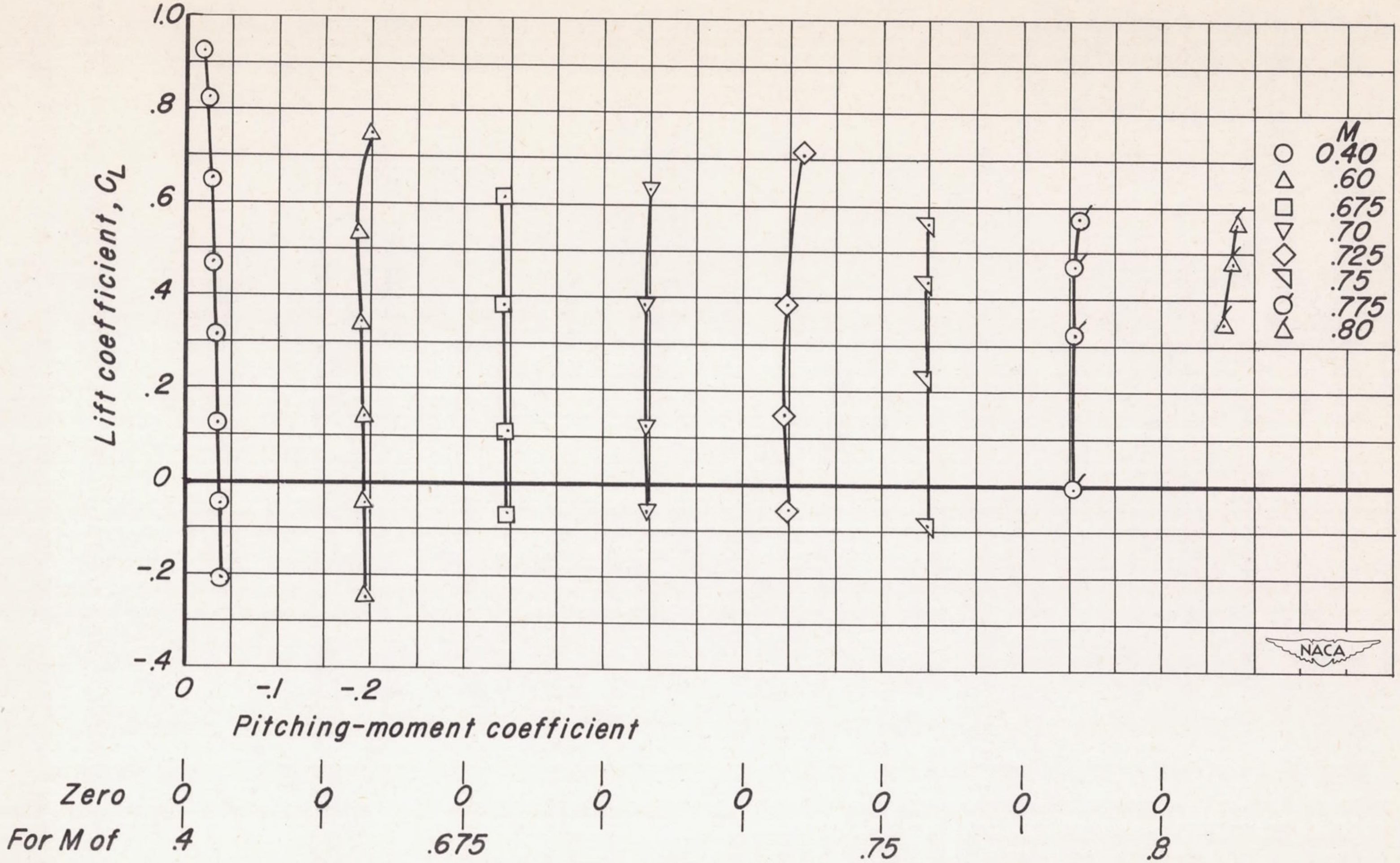

(d) Aspect ratio 6.

Figure 6.- Concluded.

CONFIDENTIAL

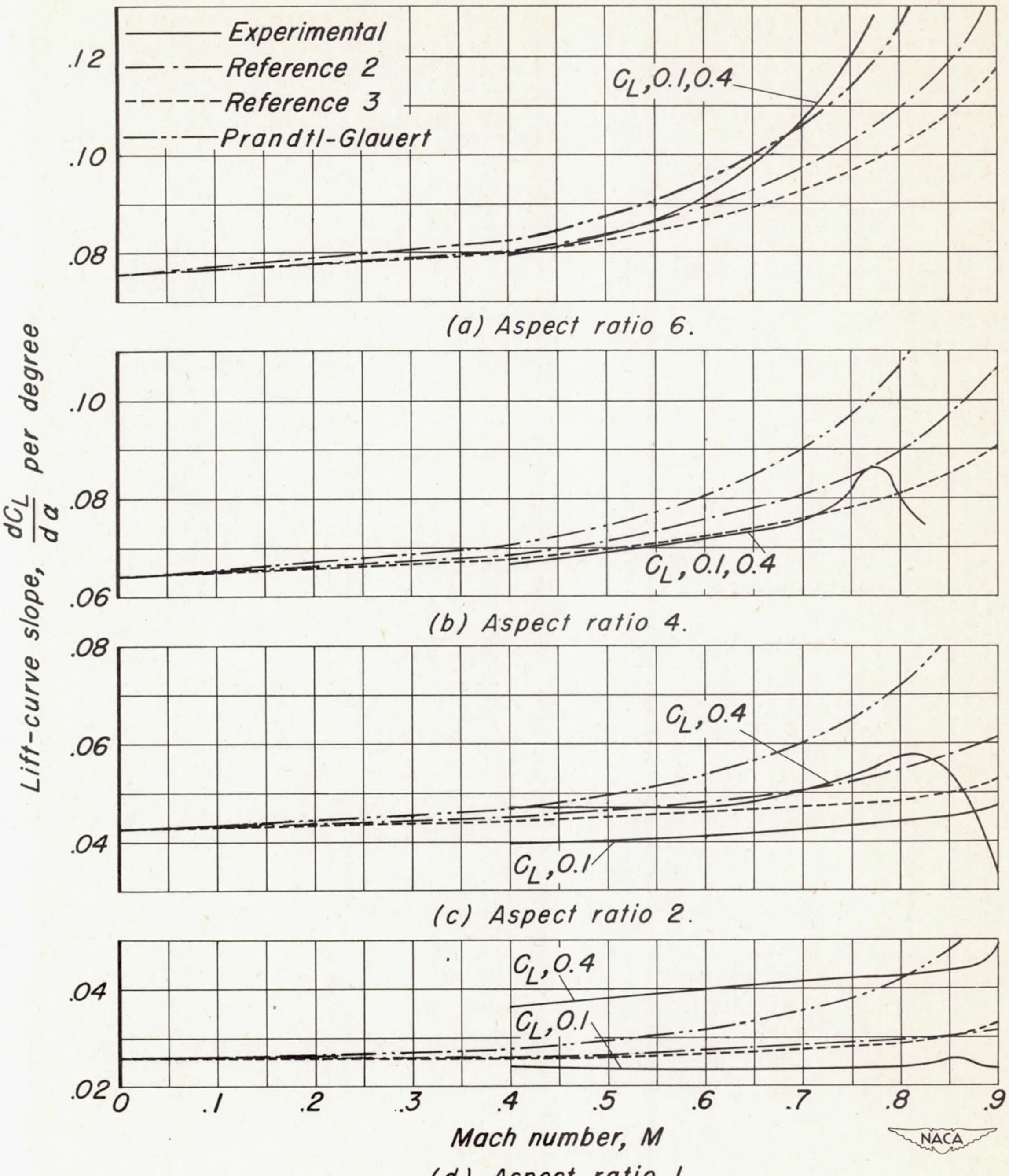

Figure 7.– Experimental and theoretical variation of lift-curve slope with Mach number.

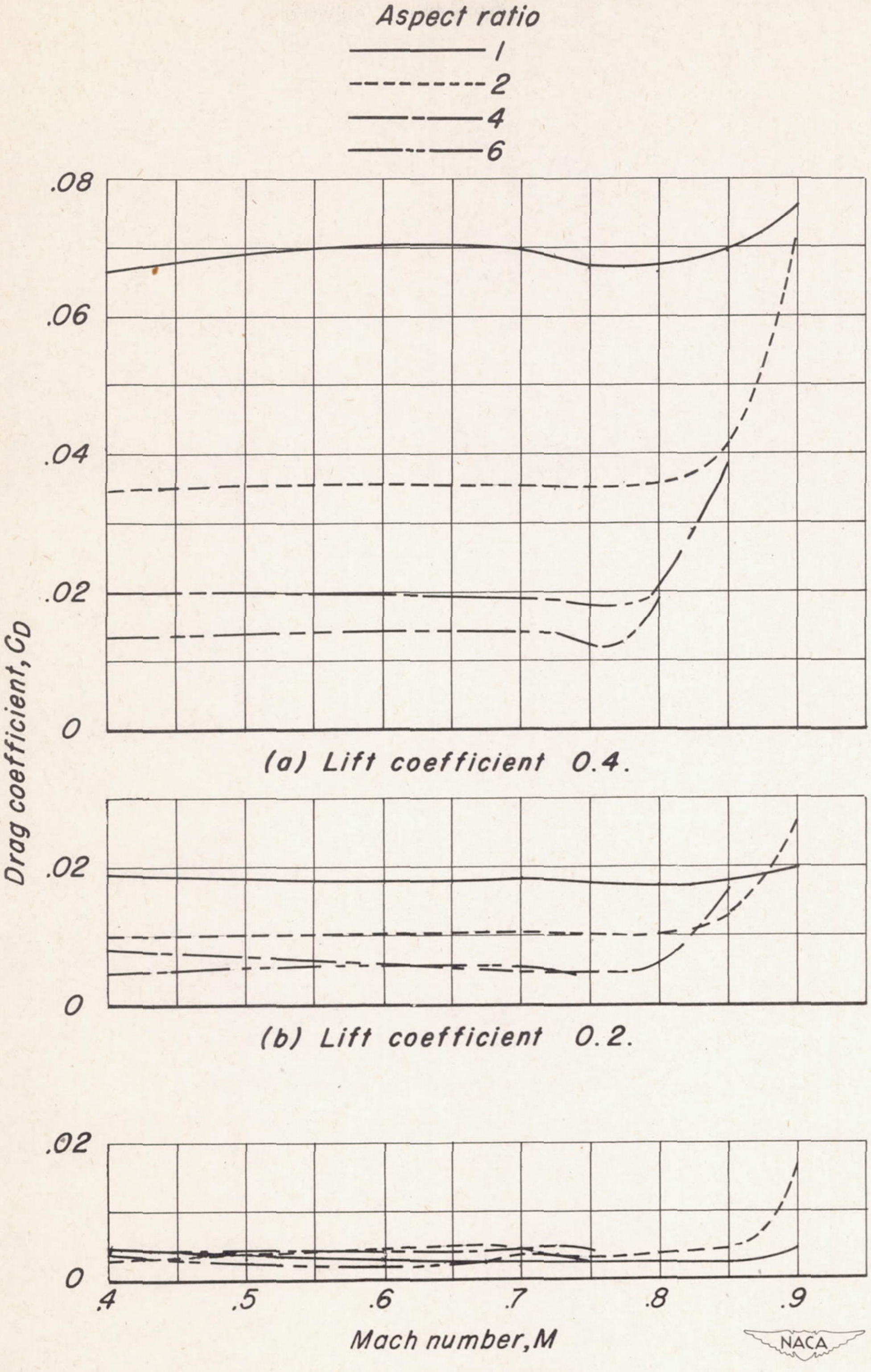

(c) Lift coefficient 0.

Figure 8.– Variation of drag coefficient with Mach number.

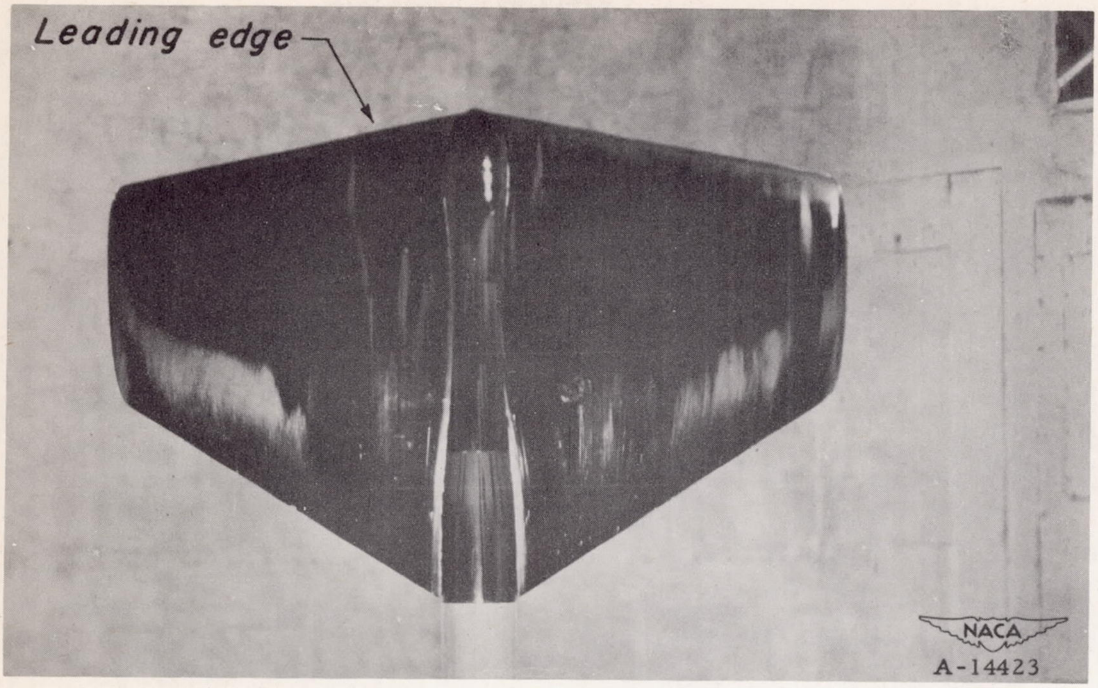

(a) Transition as it appeared during a test.

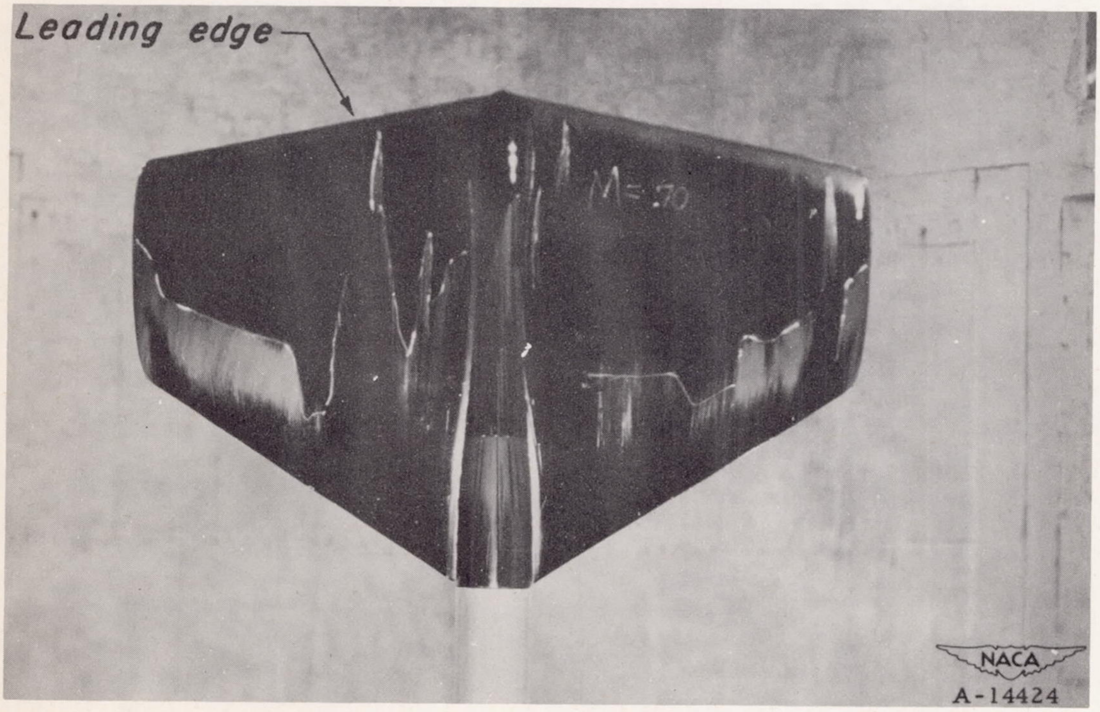

(b) Transition outlined in chalk.

Figure 9.- Typical transition on the aspect-ratio-2 wing as indicated by liquid-film evaporation.

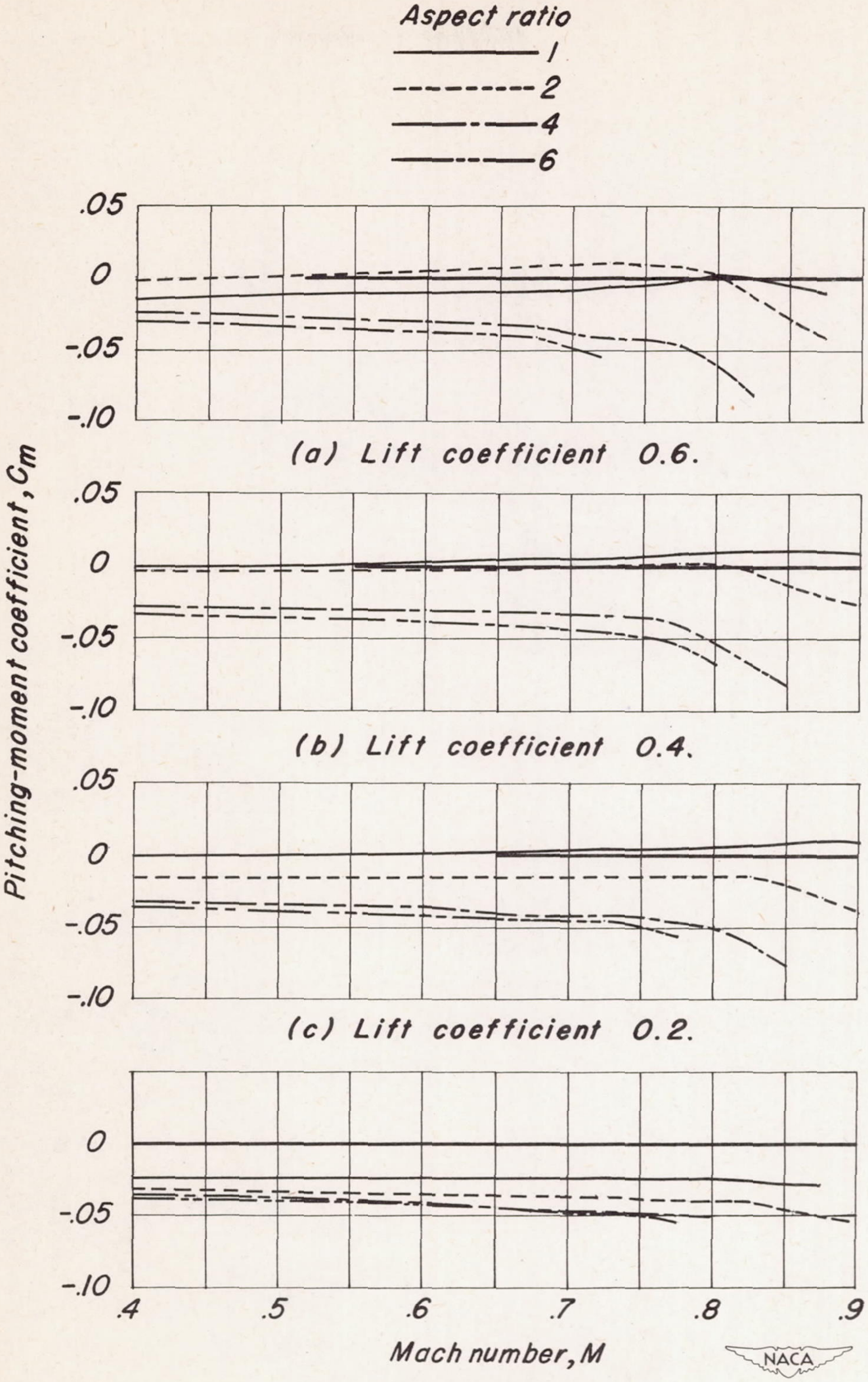

(d) Lift coefficient 0.

Figure 10.– Variation of pitching-moment coefficient with Mach number.

NACA-Langley - 2-3-50 - 275